ELSEVIER

Biophysical Chemistry 106 (2003) 111–123

Biophysical Chemistry

www.elsevier.com/locate/bpc

MD simulation of a plastocyanin mutant adsorbed onto a gold surface

Anna Rita Bizzarri*, Giulio Costantini, Salvatore Cannistraro[1]

Unita' INFM, Dipartimento di Scienze Ambientali, Universita' della Tuscia, Viterbo I-01100, Italy

Received 14 February 2003; received in revised form 23 May 2003; accepted 28 May 2003

Abstract

MD simulation of plastocyanin, an electron transfer protein, adsorbed onto a gold surface, has been performed for 10 ns. Starting from the crystallographic structure of a poplar plastocyanin mutant engineered with the insertion of a disulfide bridge, the protein has been anchored to a gold substrate modeled by a cluster of three layers in the Au⟨111⟩ configuration. A number of significant structural and dynamical properties of the protein molecule, covalently bound through either one or two sulfur atoms to the gold surface, has been extracted and compared with those of the free protein. Attention has been paid to investigate the dynamical aspects putatively related to the electron transfer process. In particular, the cross-correlation function between specific active site vibrations and all the other protein atom motions and the principal component analysis have been calculated in order to put into evidence dynamical correlation of some functional relevance. The results are discussed also in connection with related experiments.

Keywords: MD simulation; Hybrid electron transfer systems; Bioelectronic devices

1. Introduction

Recently, electron transfer (ET) proteins, chemisorbed onto gold substrates, have attracted large attention even for their possible application in biomolecule-based electronic components [1–3]. The strengths associated with utilizing biomolecules in such devices reside largely in their capacity for self-assembly, specific surface recognition and a structure designed for efficient electron transfer. Native, or suitably engineered, thiol groups and disulfide bonds are mainly used to achieve a stable immobilization as well as exploitable ET pathways [4]. Among different experimental approaches, scanning tunneling microscopy (STM) provides new progress in studying the ET process of these hybrid systems [5–7]. Azurin (AZ), a protein agent in redox systems, has been one of the most studied copper ET proteins, also in the perspective of building hybrid systems, in which the ET properties could be exploited to transduce chemical signals [8–13]. With the same aim, more recently, a mutant of poplar plastocyanin (PC), an ET protein similar to AZ, has been engineered by introducing a surface disulfide

*Corresponding author. Tel.: +39-0761-357027; fax: +39-0761-357119.

E-mail address: bizzarri@unitus.it (A.R. Bizzarri).

[1] http://www.unitus.it/biophysics/

0301-4622/03/$ - see front matter © 2003 Elsevier B.V. All rights reserved.
doi:10.1016/S0301-4622(03)00156-X

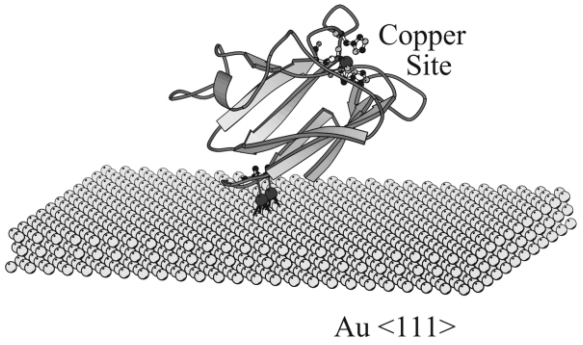

Fig. 1. Schematic representation of PCSS anchored onto a Au⟨111⟩. Each of the two protein sulfurs is engaged in covalent bonds with three gold atoms (see text).

bridge opposite to the active site [14]. It has been shown that the resulting mutated structure (PCSS) retains the spectroscopic features of the wild type structure and likely, the ET properties [14,15]. PCSS covalently binds to a gold surface through the disulfide bridge (see Fig. 1) and STM images of immobilized PCSS seem to indicate that the copper active site is involved in the ET process. Furthermore, scanning tunneling spectroscopy at the level of single molecule has revealed an intriguing rectifying-like behavior; such a peculiar molecular conduction having been detected also in air and deserving possible applications in hybrid devices [16].

We aimed, therefore, at modeling the adsorption and the interaction of the mutated PCSS at a gold surface to get more insights about the structure and dynamical features of this immobilized system and their possible implications with the ET process. In this connection, it should be stressed that while self assembled monolayers of thiol containing small organic molecules on gold surfaces [4,17–21] have been widely studied, by ab initio and MD simulation approaches, no similar information is available, to the best of our knowledge, about proteins. Only a Brownian dynamics study has been reported on a physically adsorbed protein [22]. However, MD simulations have emerged as useful means, complementary to various experimental techniques, to provide structural and dynamical properties of protein systems. In particular, MD simulations have been widely employed by some of the authors to investigate the structural, dynamical and ET properties of wild PC [23–25]; the effect of introducing a disulfide linkage-bond in poplar PC has also been studied [26].

Here, we report MD simulations of PCSS adsorbed onto a gold substrate, which have been performed after having covalently anchored the protein either with one or two sulfurs to the gold surface. As the first stage of analysis, we have focussed our attention to dry systems. In this respect, it should be mentioned that many STM and atomic force microscopy (AFM) studies on protein systems adsorbed onto metal substrates are performed, in air or even in vacuo, on dry samples [27,28].

The potential energy, the root mean square displacements (RMSD) and the gyration ratio from the initial structure of both the adsorbed systems have been monitored during 10 ns of MD simulation and compared with those of free PCSS. The orientation and precession of the protein macromolecule about the normal to the gold surface have been investigated during the MD simulated trajectories for both of the differently anchored systems. Additionally, the height of the macromolecule with respect to the gold substrate has been calculated for a set of trajectories and the corresponding histograms have been extracted. Finally, the cross-correlation function between the Cu–S(Cys84) bond distance and each protein atom motions and the principal component analysis (PCA) have been performed along the MD trajectory. This analysis shows a stability of both the anchored systems up to 10 ns. In addition, it reveals the existence of a dynamical correlation between the copper active site and protein regions far from it, including the anchoring region. These results are also discussed in connection with related experiments.

2. Computational methods

MD simulations have been performed by using the CHARMM package [29] including a standard molecular mechanics potential form. The local interactions include harmonic bonds, angles, improper torsions and dihedral angles. The long-range interactions include Lennard–Jones potential

and electrostatic potential between atom-based charges [29]:

$$V = \sum_{\text{bonds}} k_r(r-r_0)^2 + \sum_{\text{angles}} k_0(\theta-\theta_0)^2 + \sum_{\text{impropers}} k_\omega(\omega-\omega_0)^2 + \sum_{\text{dihedrals}} k_\phi \times [1+\cos(n\phi-\phi_0)] + \sum_{\text{non-bonded pairs}} \left(\frac{A_{ij}}{r_{ij}^{12}} - \frac{B_{ij}}{r_{ij}^{6}}\right) + \sum_{\text{non-bonded pairs}} \frac{q_i q_j}{r_{ij}} \quad (1)$$

Parameters for protein atoms are taken from CHARMM27 force field [30]. Initial coordinates of PCSS have been taken from the X-ray structure, at 0.16 nm resolution, of the mutant poplar PC bearing a disulfide bridge introduced by replacing Ile21 and Glu25 by two cysteines (1JXG entry of Brookhaven Protein Data Bank) [15].

PC is an eight-stranded anti-parallel β-barrel macromolecule with a copper atom liganded by the side-chains of two histidine (His37 and His87), a cysteine (Cys84) and a methionine (Met92) in a peculiar, tetrahedral geometry [31] (see Fig. 1). With the exception of the copper ligands His37, Cys84, His87, all the ionizable residues are assumed to be in their fully charged state, according to the pH value. As in previous works, a covalent bond approach for the copper site has been adopted [23,32,33]. In particular, the copper has been considered to be bound to three ligands (two nitrogens from His37 and His87, respectively, and one sulfur from Cys84), while the much weaker interaction of copper with the sulfur from Met92 has been treated by a non-bonded approach [34]. The partial charges for the copper and its ligand residues have been modified by a linear interpolation of the standard CHARMM charges between the protonated and the un-protonated residues to match the redistribution of the charges in the residues as due to the reduction of the copper charge from +2 to +0.98, by following Ref. [33]; such kind of approach having allowed us to reliably reproduce the experimental main vibrational features of PC [32]. Additionally, we remark that these charges are rather similar to those recently obtained by quantum calculations [35,36].

Starting from the crystallographic structure, to appropriately release the conformational stresses and the steric constraints as due to the presence of the gold substrate, the minimization of the PCSS has been carried out with a combination of three different algorithms: 500 steps with the steepest descent, 500 steps with the conjugate gradient and finally, 1000 steps with the adopted basis Newton–Raphson minimization. An equilibration procedure has been then performed by rising the temperature of the system from 0 K to 300 K with increments of 5 K every 0.2 ps, by assigning the atomic velocities according to a Maxwellian distribution. Subsequently, a MD simulation at 300 K has been carried out for 200 ps with a Gaussian velocity reassignment when the temperature deviated of more than 10 K from the assigned temperature.

After that, the dynamics of the system have started by sampling at intervals of 0.1 ps for 10 ns; a careful scaling down of the velocity during the simulations having been performed [37,38]. The Shake constraint algorithm [39] has been used for all hydrogens. A cut-off ratio of 11 and 13 Å has been used for the Lennard–Jones and the electrostatic energy functions, respectively. The MD simulations of free PCSS have been conducted in the micro canonical ensemble (NVE). In order to assess a good exploration of the configuration in the phase space, a scaling down of the velocity has been performed during the simulation. To model the Au(111) surface, the gold atoms have been arranged hexagonally into a cluster of three layers each one with 22×25 atoms; the charge of the gold atoms has been put to zero. The nearest neighbor distance has been assumed to be 2.88 Å and the positions of the gold atoms have been fixed during all the simulations.

According to experiments, PCSS is expected to be covalently anchored to the gold surface by involving the sulfurs of the engineered S–S bridge (see Fig. 1) [14]. Since one or both sulfurs might be involved in the anchoring of the protein to the substrate, two different systems have been investigated. First, to increase the external accessibility of the sulfurs, monitored by the Lee and Richards algorithm [40], the disulfide bridge has been broken in agreement with the experimental evidence pointing out that chemisorption occurs after the

Table 1
Force field parameters describing the interactions between PCSS and the gold surface [43]. These interaction parameters are added to the CHARMM27 all-atoms interactions

	Harmonic bond interaction		
	r_0(Å)	k_r(kcal/mol Å^2)	
Au–S	2.531	198	
S–C	1.836	205	
	Harmonic angle interaction		
	θ_0(deg)	k_θ(kcal/mol)	
Au–S–C	109	46.347	
	Dihedral angle interaction		
	ϕ_0(deg)	k_ϕ(kcal/mol)	n^*
Au–S–C–C	180	0.31	2
S–C–C–C	−19	0.22	2
	Lennard–Jones interaction**		
	r_{min}(Å)	E_{min}(kcal/mol)	
Au	2.0736	0.078	

* multiplicity of dihedral angles.
** see ref. [43].

S–S bond dissociation [4,41]. After a minimization, an accessible surface of approximately 2 Å^2 for Cys25 sulfur has been obtained. Subsequently, a minimization of the protein approaching the gold surface has been carried out. Protein–gold interactions have been described by Lennard–Jones potentials; with the interaction parameters being reported in Table 1. At the end of this further minimization, the Cys25 sulfur exhibits an accessibility of approximately 17 Å^2. A covalent bond between this sulfur and the gold surface has been then established. In particular, the sulfur atom has been bound with three-fold fcc hollow site gold atoms, placed at the center of the area surface in agreement with Ref. [42]; such a geometrical arrangement having been shown to be energetically more favorable [19]. The second sulfur of the bridge has been saturated with a hydrogen atom as a standard cysteine; such a configuration having labeled as PCSS-I. The parameters used to describe the gold protein interactions are reported in Table 1 [43].

In the configuration labeled as PCSS-II, both Cys25 and Cys21 sulfurs have been covalently anchored to the gold substrate. Starting from the PCSS-I configuration, to attach the second sulfur (Cys21) to the gold surface, the disulfide bridge has been re-established and the system has been minimized. An accessible surface of 14 and 21 Å^2 for Cys21 and Cys25 sulfurs, respectively, has been obtained. After the breaking of the disulfide bridge, the Cys21 sulfur has been anchored at a fcc three-fold hollow site of the gold. A schematic picture of the PCSS bound to the gold surface by two covalent bonds is shown in Fig. 1. This configuration will be referred to as PCSS-II in the following.

For both the systems, a minimization and an equilibration procedure has been started, followed by 10 ns of data collection (simulation PCSS-I and simulation PCSS-II). To identify the correlated atomic motions, the MD trajectories of PCSS, PCSS-I and PCSS-II have been analyzed according to the PCA or essential dynamics [44,45]. This approach aims at identifying a new reference frame such that only a subset of coordinates, usually on the order of a few percent of the total, is sufficient to describe the overall dynamics of the system. The remaining degrees of freedom, corresponding to constrained harmonic oscillations, can be neglected. Such a method is based on the diagonalisation of the covariance matrix, built from the atomic fluctuations in a MD trajectory from which overall translational and rotational motions have been removed:

$$C_{ij} = \langle (X_i - X_{i,0})(X_j - X_{j,0}) \rangle \quad (2)$$

where X are the x-, y- and z-coordinates of the atoms fluctuating around their average positions X_0 and where $\langle ... \rangle$ denotes an average over time.

To construct the protein covariance matrices, we have used the C_α atom trajectories, including the copper atoms. Upon diagonalisation of the covariance matrix, a set of eigenvalues and eigenvectors is obtained. The eigenvectors of the covariance matrix correspond to directions in a $3N$ dimensional space (where N is the number of C_α atoms including the copper atom) and motions along single eigenvectors correspond to concerted fluctuations of atoms. The eigenvalues represent the total mean square fluctuation of the system along the corresponding eigenvectors. If the eigenvectors are ordered according to decreasing eigenvalues,

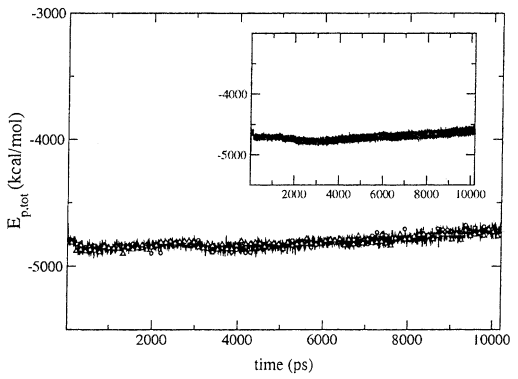

Fig. 2. Temporal evolution of the total potential energy, along a 10 ns MD trajectory for the PCSS-I (circles) and PCSS-II (triangles) systems. Inset: temporal evolution of the total potential energy for free PCSS.

the first one describes the largest scale correlated motions, whereas the last one will correspond to small-amplitude vibrations [44].

3. Results and discussion

The potential energy trend observed during 10 ns of MD simulation of both the adsorbed PCSS-I and PCSS-II systems are shown in Fig. 2. For comparison, that of free PCSS is also plotted (inset of Fig. 2).

After a short initial time, the potential energies of free PCSS, PCSS-I and PCSS-II appear to be practically constant in time with a small drift (see Table 2); the energy of free PCSS appearing to be slightly higher than that of the bound protein systems. Such a trend seems to indicate that the adsorption of the protein to the gold substrate does not substantially affect the stability of the system.

From Table 2, it is inferred that high values for the standard deviation are also detected for the total potential energy of PCSS-II and PCSS-I. As long as the spread of the potential energy reflects the sampling of the conformational substates and local minima of the protein energy landscape [46–48], such a behavior is indicative of the fact that an exploration of the energy landscape also occurs for the immobilized systems. In addition, the slightly lower value for the standard deviation of PCSS-II with respect to PCSS-I, suggests that the binding of the protein to the gold surface by two sulfurs might yield some restriction in the energy landscape region accessible to the protein during its dynamical evolution.

An analysis of the Lennard–Jones energy, separately reported in Table 2, shows an increase of this energy component, with respect to free PCSS, for both the immobilized systems; such an effect being particularly evident for PCSS-I. Moreover, since the Lennard–Jones energy is essentially made up by protein atom–atom and protein–atom gold–atom interactions, the contribution as due to the protein–gold interaction has been extracted. We note from Table 2 that the Au–PCSS Lennard–Jones energy constitutes a significant part of the total Lennard–Jones energy for both the immobilized systems; such a contribution to the total Lennard–Jones energy is more significant in PCSS-I than in PCSS-II.

To get further insight into the effect of gold-adsorption on the structural and dynamical feature of the protein, we have calculated the RMSD from the equilibrated structure. The RSMDs of all the protein atoms as a function of time are plotted in Fig. 3 for both PCSS-I and PCSS-II, and for free PCSS in inset of Fig. 3. During 10 ns of MD simulation run, the RMSDs of both the PCSS systems anchored to the gold substrate undergo a few jumps. In particular, the most significant jumps

Table 2
Average value, standard deviation and drift, expressed in kcal mol^{-1} ns^{-1}, of total potential energy and of the Lennard–Jones components for PCSS, PCSS-I and PCSS-II, as extracted from a 10 ns trajectory. The drift has been calculated from a linear regression over the total trajectory

	Mean	Standard deviation	Drift
Total potential energy (Kcal/mol)			
PCSS	−4704	53	0.013
PCSS-I	−4810	54	0.015
PCSS-II	−4814	44	0.012
Lennard–Jones energy			
PCSS	−71	27	0.004
PCSS-I	−16	18	−0.0012
PCSS-II	−59	26	0.004
Au-PCSS Lennard–Jones energy			
PCSS-I	−8	0.9	-6×10^{-5}
PCSS-II	−12	1.2	0.0002

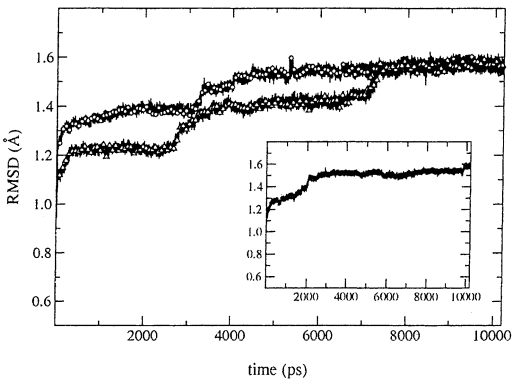

Fig. 3. RMSD from the starting structure of PCSS-I (line and circles) and PCSS-II (line and triangles) along a 10 ns MD trajectory. Inset: RMSD of the free PCSS. The RMSD have been obtained by averaging over all the protein atoms.

are observed at approximately 3.1 ns, for PCSS-I, and at 3.0 ns and 7.2 ns for PCSS-II, respectively, and at approximately 2.1 ns for free PCSS. In order to investigate if these jumps arise from conformational changes, we have analyzed the protein conformation before and after these transitions. The most relevant changes appear at 2.5–4.0 ns jump of PCSS-II. Indeed, Fig. 4, showing a superposition between the structure averaged over a 0.5 ns time interval before and after the jump detected for the PCSS-II system, reveals small changes in correspondence of the turns T1 and T8, of the S1 strand and of the α-helix. However, the main protein structure is preserved; a similar behavior occurring for other jumps.

A comparison between the main-chain C_α traces of PCSS-I, PCSS-II and of free PCSS is plotted in Fig. 5. The structures have been obtained by averaging all the atom positions over the entire simulation. Generally, we note that the overall protein structure is substantially preserved upon adsorbing the macromolecule onto the gold substrate, though some small structural changes can be put into evidence. At a visual inspection, the most significant differences are detected at the turns T1, T3, T5 and T8 and at the β-strand S4 for PCSS-I. The changes at T3 and S4, close to the anchored protein sulfur, are reasonably due to the direct involvement of these regions into the binding to the gold atoms. Concerning PCSS-II, we again observe changes at T3, T5, T8, S4 and, in addition, at the β-strand S3. The region closer to the gold anchorage site exhibits larger conformational changes in comparison with PCSS-I. This points out that the presence of two anchoring points can result in more relevant structural and dynamical constraints on the protein structure. Furthermore, small structural changes at the copper active site can be also detected for both PCSS-I and PCSS-II.

Additional information about the protein conformation evolution during the dynamics can be obtained by analyzing the gyration ratio R_g: values for R_g of (12.395 ± 0.044)Å for the free PCSS, and of (12.373 ± 0.012)Å and (12.547 ± 0.031)Å for PCSS-I and PCSS-II, respectively, by averaging over 10 ns. According to our previous work, the gyration ratio of free PCSS is not significantly different from that of wild PC [26]. Moreover, it turns out that PCSS-I shows a R_g value practically

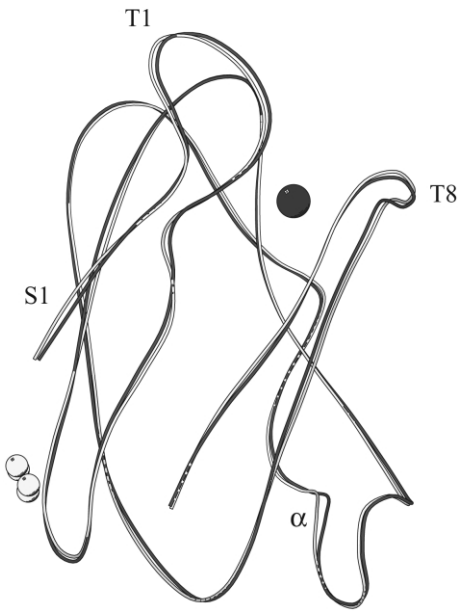

Fig. 4. Main-chain C^α traces of the PCSS-II as obtained from the time-averaged structure over 2.0–2.5 ns (light grey) and 4.0–4.5 ns time interval (dark grey). The T1 and T8 turns, the β-strand S4 and the α-helix are the region where the most significant differences between the two structures are detected. The copper atom and the Cys21 and Cys25 sulfur are shown.

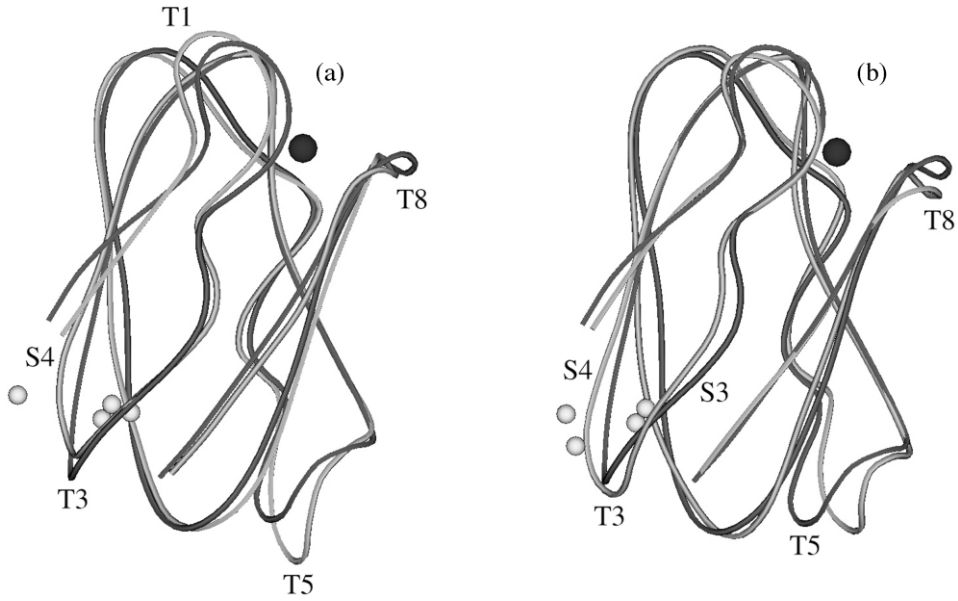

Fig. 5. Main-chain C^{α} traces, time-averaged over 10 ns, of free PCSS (dark grey), of PCSS-I [light grey (a)] and PCSS-II [light gray (b)] structures, respectively. The turns (T1, T3, T5 and T8) and β-strands (S3 and S4) are the regions where the most significant changes are observed. The copper atom and the Cys21 and Cys25 sulfurs are shown.

equal to that of free PCSS; a slightly higher value appearing for PCSS-II.

An interesting aspect, which might be relevant in connection with some experimental results, is the overall orientation of the macromolecule with respect to the gold substrate. Actually, topological information as obtained by AFM, on immobilized protein systems are related to the orientation and structural arrangements of the macromolecular at the gold surface [13,49]. At the same time, since the copper active site plays a crucial role in the mechanisms regulating the ET process [34], the position of the copper and the related electron levels are expected to be relevant for the protein–gold ET paths in these hybrid systems; these aspects having been investigated also by STM [11,12]. On such a ground, we have described the protein orientation with respect to the gold surface by θ and ϕ angles as depicted in Fig. 6: θ is the angle that the axis $\vec{p}$, joining the sulfur of Cys25 and the copper atom, forms with the normal to the gold surface; ϕ is the precession of $\vec{p}$ about the gold surface normal. The trend with time of θ and ϕ, calculated during the MD trajectory, are plotted, for both the PCSS-I and PCSS-II systems, in Fig. 6a and Fig. 6b, respectively. We note that in both systems a significant deviation of $\vec{p}$ from the normal axis is registered. In addition, the mean value of θ is smaller for PCSS I than for PCSS-II (see legend of Fig. 6); this means that the $\vec{p}$ axis is closer to the normal for the protein system anchored by a single bond. Such a behavior could find a correspondence with the lower Lennard–Jones energy calculated in this case and might be indicative of a less extensive contact between the protein atoms and the gold surface. However, anchoring the protein with both sulfurs drives the $\vec{p}$ axis closer to the gold surface plane (higher θ).

Concerning ϕ, PCSS-I and PCSS-II show rather similar average values. A much larger variability is observed for the PCSS-I in comparison with PCSS-II (see legend of Fig. 6). In addition, it is interesting to note the presence, in both the systems, of fast oscillations to which slower oscillations are overimposed; the origin of such an effect being not clear.

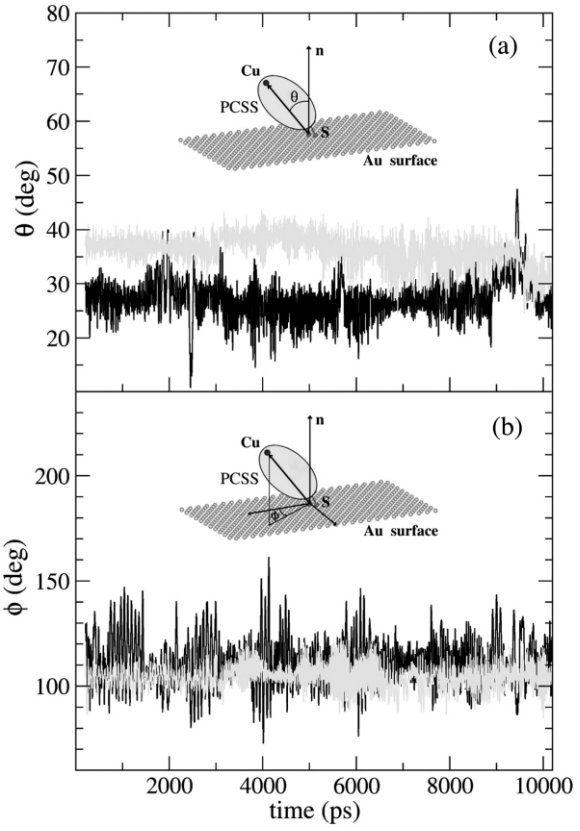

Fig. 6. Temporal evolution, along a 10 ns MD trajectory, of the θ (a) and ϕ (b) angles describing the orientation and the precession, respectively, of the protein $\vec{p}$ axis with respect to gold surface normal, for the PCSS-I (dark gray) and PCSS-II (light gray). The average value and the standard deviation of θ are $(27\pm4)^\circ$ and $(36\pm3)^\circ$ for PCSS-I and PCSS-II, respectively. The average values and the standard deviations of ϕ are $(112\pm12)^\circ$ and $(105\pm6)^\circ$ for PCSS-I and PCSS-II, respectively. The inset depicts the θ and ϕ angles.

These results can provide some hints in the interpretation of the experimental topological data, as obtained by AFM, of immobilized proteins. In this connection, the protein is represented by an ellipsoid centered at the center of mass of the protein and oriented as its main inertia axes (as an example see inset of Fig. 6). The ellipsoid, evaluated from the MD simulated trajectories, gives an overall representation of the macromolecule thus providing an appropriate description of the protein height in order to be compared with the related data from topological AFM [13,50]. The ellipsoid and its corresponding height over the gold substrate have been extracted from the MD simulated trajectories by sampling structures every 10 ps. The histograms of the heights, as obtained by 1000 structures, are shown in Fig. 7. From this figure, it shows that a single mode distribution is registered for both systems. The mean values are, in both cases, close to that expected for the crystallographic data by assuming that protein is anchored to gold via the disulfide bridge ($h \sim 3$ nm). However, we note that PCSS-I is characterized by a mean value slightly higher than that of PCSS-II (see Fig. 7). Such a finding is consistent with the previous results, showing that the protein anchored by a single bond can assume, on average, a configuration closer to the normal to the surface. For both systems, a spread of heights is registered (see Fig. 7). Generally, this means that the macromolecule dynamically samples its accessible conformations; assuming a variety of arrangements, and then of heights, with respect to the gold substrate. However, we note that PCSS-I is characterized by a wider distribution in comparison with PCSS-II. As a consequence, molecules covalently bound to gold through one sulfur atom show slightly higher flexibility than molecules anchored via two covalent bonds. By

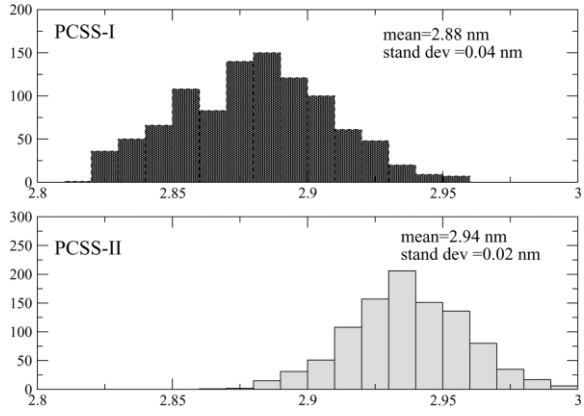

Fig. 7. Statistical analysis of the molecular height above the Au(111) substrate, as extracted from the MD simulated trajectories for PCSS-I and PCSS-II. The vertical dimension of proteins has been estimated from 1000 molecules sampled every 10 ps of the MD simulated trajectory.

comparing these results, we note that the height distribution, as extracted by MD simulation, results markedly narrower than that derived by AFM [50]. This finding can be explained by taking into account the stress exerted by the tip on the biomolecule during the AFM measurements. Indeed, even in tapping mode (in which the tip is expected not to be in a direct contact with the sample), some kind of interaction between the tip and the biomolecule can occur. However, AFM is sensitive to protein movements on a much longer time scale (at least milliseconds if we refer to tapping mode with a frequency in the range of kilohertz). Additionally, we remark that AFM data refer to a collection of molecules, likely in different starting arrangements and anchored to gold either by one or both sulfur atoms, whereas, MD simulations consider only an isolated molecule in two different anchoring situations. Nevertheless, the present MD simulations suggest that the protein, even if sampled in a restricted temporal window, can assume a variety of orientations with respect to the gold substrate.

It is well-ascertained that the ET process occurring in a protein system, results to be coupled to some nuclear motions involving atoms far from the active site [51,52]. Moreover, vibrations of ET proteins are of main concern for the functionality since they operate a fine-tuning of the redox potential and hence of the electron transfer process [51]. In this connection, the study of the dynamical behavior of PCSS, anchored to a gold substrate, is of utmost relevance to investigate if the protein retains its native dynamical and ET functional properties. In wild PC, it has been shown that some macromolecular motions, even far from the active site, along putative ET paths, are strongly correlated to the fluctuations of Cu–S(Cys84) bond distance [33]. Notably, the power spectra as extracted from the temporal fluctuations of such a bond distance during a dynamical evolution are closely similar to those detected in the resonant Raman spectra [32,33].

On such a ground, and in order to put into evidence the coupling between protein motions and the vibrations of the active site, relevant to the ET process, we have performed an analysis of the cross-correlation function of the Cartesian

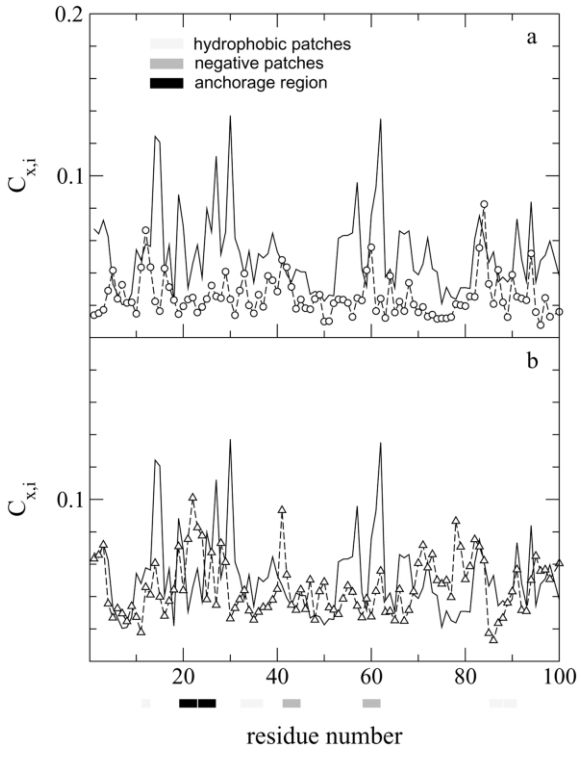

Fig. 8. Cross correlation $C_{x,i}$ as calculated from Eq. (2), for free PCSS (continuous line), PCSS-I (a) (dashed line and circles) and PCSS-II (b) (dashed line and triangles), averaged over 10 ns MD simulation trajectory, plotted vs. backbone atoms (N, C^{α}, C and O). Some of the structural elements involved in the ET process are shown.

motions of each protein atom with the Cu–S(Cys84) bond distance x [33]:

$$C_{xi,\alpha} = \frac{\left\langle (r_{i,\alpha} - \langle r_{i,\alpha}\rangle)(x - \langle x\rangle)\right\rangle}{\left[\left\langle (r_{i,\alpha} - \langle r_{i,\alpha}\rangle)^2\right\rangle\right]^{1/2}\left[\left\langle (x - \langle x\rangle)^2\right\rangle\right]^{1/2}} \qquad (3)$$

where $r_{i,\alpha}$ designates one of the three α coordinates of the position of the atom i. A single atomic value can be obtained by means of the geometrical average of $C_{x,i}$. Fig. 8 shows the $C_{x,i}$ as a function of the backbone atoms, extracted by averaging over a 10 ns MD trajectory, for free PCSS, PCSS-I and PCSS-II.

Free PCSS reveals high values for $C_{x,i}$ throughout the protein residues. In particular, the most evident peaks are detected at Phe14, Cys25, Ile27,

Met57, Leu62, Tyr83. Generally, most of these peaks find a correspondence with those observed in wild PC by Ungar et al. [33]; such an agreement confirming that the insertion of a disulfide bridge does not alter the ET properties of the system. Indeed, some of these peaks involve protein residues, which are known to be implied into the ET process. In particular, the peak at Phe14, spatially close to Leu12, involves the PC hydrophobic patch, while the peak at Leu62 is located around the negative patch; both these regions being relevant for binding reaction partners as well for assisting the ET process [34]. Moreover, the strong vibrational coupling of Tyr83 is consistent with the hypothesis that this residue could be a main element of the ET path from the PC partner cytochrome *f* [34]. In addition, it is worth noting that a strong correlation between the functional active site and the disulfide bridge is observed. Dynamical correlation extending over large distances should be considered quite reasonably in the light of the experimental finding, showing that the spectroscopic features of copper proteins are sensitive to the protein amino acid composition up 12 Å from the copper metal [52].

Regarding the $C_{x,i}$ cross-correlation for PCSS I, most of the peaks observed in free PCSS are suppressed. However, the peaks around Leu14, Glu61 and Tyr83 are still detected even if with a lower intensity. An additional peak at Phe41 is observed. Notably, the protein region containing the engineered residues Cys21 and Cys25 exhibits lower values for $C_{x,i}$ with respect to free PCSS. In particular, a small peak is detected at the Cys25 gold anchoring site, while practically no correlation is detected at the Cys21 residue. Such a behavior indicates that the removal of the covalent disulfide bridge, in connection with the insertion of a single protein gold anchoring bond, can significantly modulate the dynamical correlation properties of this region with the active site.

On the contrary, the $C_{x,i}$ trend for PCSS-II appears qualitatively rather similar to that of free PCSS; three additional major peaks, located at residues Ser22, Phe41 and Gly78, can be detected. At the same time, lower values in comparison to free PCSS are observed around the residues Ser17, Cys25, Met57 and Glu60. It is worth noting that the anchoring region, now involving two protein sulfur gold bonds, exhibits high values for $C_{x,i}$. Such a finding could indicate that the dynamical cross-correlation of the gold–protein anchoring region with the active site, is strongly dependent on the structure of the binding site. However, the fact that the double bond anchorage is dynamically coupled to the copper active site suggests that it might play a role in the ET process toward the gold electrode. This could be of some relevance for bioelectronic application in hybrid systems, as a number of STM experiments seem to indicate [11–13,16]. Indeed, in these hybrid systems, the covalent anchorage of the protein to the gold surface is expected to take part in the ET pathway joining the copper active site to the metallic substrate; even if electric field fluctuations should also be taken into considerations.

To provide further information about the effect of anchoring the macromolecule to a gold surface on its overall motions also in connection with its ET functionality, we have applied the PCA to the C_α atoms of all the analyzed systems. Similar to that observed in our previous simulations for wild type and mutated plastocyanins [24,26], it has been found that approximately 80% of the total protein motions are described by the first 30 eigenvectors (data not shown). The absolute value of the components of the first four eigenvectors of PCSS, PCSS-I and PCSS-II are shown in Fig. 9. For free PCSS, we observe correlated motions, mainly involving turns (see Fig. 9). In particular, in the first eigenvector, concerted motions among T3, T4 and T5 are detected. Similarly, in the successive eigenvectors, concerted motions involving the turns T3, T7, T1, T3, T4 and T8 are evident. Generally, such a behavior is qualitatively similar to that observed in fully hydrated PCSS and wild type PC [24,26].

At a visual inspection, the absolute values of the first eigenvectors of both PCSS-I and PCSS-II reveal concerted motions involving a larger portion of the macromolecule with respect to the free PCSS. Indeed, for both the systems, we note large peaks in correspondence of regions containing both turns and β-strands. Furthermore, it is interesting to remark that by comparing the first three eigenvectors of PCSS-I and PCSS-II, the main peaks

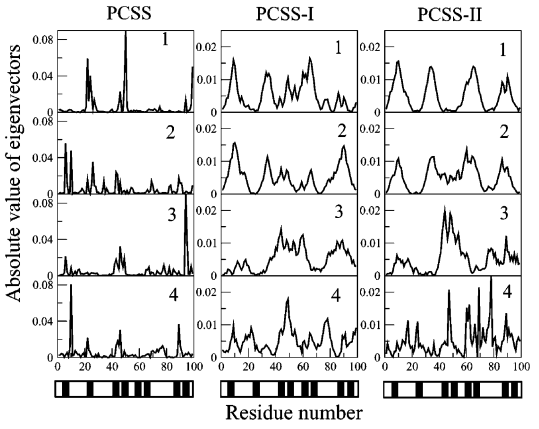

Fig. 9. Absolute values of the component of the first four eigenvectors for PCSS, PCSS-I and PCSS-II as a function of residue number. The positions of the turns T1, T3, T4, T5, T6, T7 and T8 in the secondary structure are also shown.

are approximately located at the same position. This suggests that anchoring the protein to the gold substrate might result in the selection of large respiratory motions; irrespective of the fact that one or both the protein sulfurs are covalently bound to gold.

Concerning the first two eigenvalues of PCSS-I and PCSS-II, we note the appearance of correlated motions in the 1–19, 27–41, 54–72 and 82–97 residues. These motions involve all the hydrophobic patch and a large part of the negative patch; with both of these patches playing a role in the binding with ET partners and being rather close to the active site [34]. At the same time, the copper ligand residues are also found to be involved in the correlated motions of these eigenvalues. In the third eigenvalue of PCSS-I and PCSS-II, a marked peak involving the 38–62 residues, at which the negative and the hydrophilic patch is located, can be detected. Finally, it is interesting to note that the fourth eigenvalue exhibits many sharp peaks with a behavior approaching that observed for free PCSS; such a trend being more evident for the successive eigenvectors (not shown). These results suggest that a protein anchored to a gold substrate selectively enhances peculiar concerted motions in the first eigenvectors, while higher eigenvectors show correlated motions rather similar to those detected in the free system; the latter motions being likely involved in the ET functionality. Accordingly, it could be hypothesized that the motions peculiar to the ET process could be still active in the immobilized systems.

4. Conclusions

The present study constitutes the first MD simulation of a protein, covalently bound to a gold substrate. Our results point out that, anchoring a disulfide engineered plastocyanin, through either one or two covalent bonds to a gold surface does not substantially alter the structural properties of the macromolecule; the overall structure appearing stable for the 10 ns MD simulation run.

The analysis of the orientation of the axis joining the binding site to the copper ion, shows a different dynamical arrangement with respect to the gold surface when anchoring by one or two covalent bonds are considered. A statistical analysis of the height of the macromolecule with respect to the gold substrate has allowed us to compare MD simulation data and topological experimental data as obtained by AFM.

Finally, the study of the Cu–S(Cys84) bond distance cross-correlation and the PCA investigations have provided us some information about the dynamical couplings relevant to the ET process and susceptible to be investigated by STM.

MD modeling of these immobilized systems could be of some help in elucidating the ET process also towards metallic electrode, whose control should constitute the first step to build hybrid systems by using ET biomolecules.

Acknowledgments

This work has been partially supported by the ‘Molecular Nanodevices’ FIRB project, ‘Single Molecule Spectroscopy’ INFM-PAIS project and the EC Project SAMBA (V Frame FET).

References

[1] J.M. Shifman, B.R. Gibney, R.E. Sharp, P.L. Dutton, Functionalized de novo designed proteins: mechanism of proton coupling to oxidation/reduction in hemo

protein maquettes, Biochemistry 39 (2000) 14 813–14 827.
[2] I. Willner, V. Geleg Shbtai, E. Katz, H.K. Rau, W. Haehnel, Integration of a reconstituted de novo synthesized hemoprotein and native metalloproteins with electrode supports for bioelectronic and bioelectrocatalytic applications, J. Am. Chem. Soc. 121 (1999) 6455–6468.
[3] G. Gilardi, A. Fantuzzi, S.J. Sadeghi, Engineering and design in the bioelectrochemistry of metalloproteins, Curr. Opin. Struct. Biol. 11 (2001) 491–499.
[4] A. Ulman, Formation and structure of self-assembled monolayers, Chem. Rev. 96 (1996) 1533–1554.
[5] J. Chen, M.L. Reed, M.A. Rawlett, J.M. Tour, Large on–off ratios and negative differential resistance in a molecular electronic device, Science 256 (1999) 1550–1552.
[6] C. Joachim, J.K. Gimzewski, Analysis of low-voltage I(V) characteristics of a single C60 molecule, Europhys. Lett. 30 (1995) (1995) 409–414.
[7] E.P. Friis, J.E.T. Anderson, Y.I. Kharkats, A.M. Kuznetsov, R.J. Nichols, J.D Zhang, et al., An approach to long range electron transfer mechanisms in metalloproteins: in situ scanning tunneling microscopy with submolecular resolution, Proc. Natl. Acad. Sci. USA 96 (1999) 1379–1384.
[8] P.B. Lukins, T. Oates, Single-molecule high-resolution structure and electron conduction of photosystem II from scanning tunneling microscopy and spectroscopy, Biochim. Biophys. Acta 1409 (1998) 1–11.
[9] G.B. Khomutov, L.V. Belovolova, S.P. Gubin, V.V. Khanin, A.Yu. Obydenov, A.N. Sergeev Cherenkov, et al., STM study of morphology and electron transport.features in cytochrome *c* and nanocluster molecule monolayers, Bioelectrochemistry 55 (2002) 177–181.
[10] J.J. Davis, H.A.O. Hill, A.M. Bond, The application of electrochemical scanning probe microscopy to the interpretation of metalloprotein voltammetry, Coord. Chem. Rev. 200 (2000) 411–442.
[11] J. Zhang, Q. Chi, Q.A.M. Kuznetsov, A.G. Hansen, H. Wackerbarth, H.E.M. Chris-tensen, et al., Electronic properties of functional biomolecules at metal/aqueous solution interfaces, J. Phys. Chem. B 106 (2002) 1131–1152.
[12] P. Facci, D. Alliata, S. Cannistraro, Potential-induced resonant tunneling through a redox metalloprotein investigated by electrochemical scanning probe microscopy, Ultramicroscopy 89 (2001) 291–298.
[13] J.J. Davis, H.A.O. Hill, The scanning probe microscopy of metalloproteins and metalloenzymes, Chem. Comm. (2002) 393–401.
[14] L. Andolfi, S. Cannistraro, G.W. Canters, P. Facci, A.G. Ficca, I.M.C. Van Amsterdam, et al., A poplar plastocyanin mutant suitable for adsorption onto gold surface via disulphide bridge, Arch. Biochem. Biophys. 399 (2002) 81–88.
[15] M. Milani, L. Andolfi, S. Cannistraro, M.Ph. Verbeet, M. Bolognesi, The 1.6 resolution crystal structure of a mutant plastocyanin bearing a 21–25 engineered disulfide bridge, Acta Cryst. D 57 (2001) 1735–1738.
[16] L. Andolfi, S. Cannistraro, G.W. Canters, J.J. Davis, H.A.O. Hill, M. Ph. Verbeet, to be submitted.
[17] J. Hautman, M.L. Klein, Simulation of a monolayer of alkyl thiol chains, J. Chem. Phys. 91 (1989) 4994–5001.
[18] H. Groenbcck, A. Curioni, W. Andreoni, Thiols and disulfides on the Au(111) surface: the headgroup-gold interactions, J. Am. Chem. Soc. 122 (2000) 3839–3842.
[19] M.C. Vargas, P. Giannozzi, A. Selloni, A.J. Scoles, Coverage-dependent adsorption of CH_3S and $(CH_3S)_2$) on Au(111): a density functional theory study, J. Phys. Chem. B 105 (2001) 9509–9513.
[20] Z. Zhang, T.L Beck, J.T. Young, F.J. Boerio, Molecular structure of manolayors from thiol-terminated polyimide model compounds on gold. 2. molecular dynamics simulations, Langmuir 12 (1996) 1227–1234.
[21] M. Tarek, K. Tu, M.L. Klein, D.J. Tobias, Molecular dynamics simulations of supported phospholipid/alkanthiol bilayers on a gold (111) surface, Biophys. J. 77 (1999) 964–972.
[22] S. Ravichandran, J. Talbot, Mobility of adsorbed proteins: a Brownian dynamics study, Biophys. J. 78 (2000) 110–120.
[23] A. Ciocchetti, A.R. Bizzarri, S. Cannistraro, Long term molecular dynamics simulation of copper plastocyanin in water, Biophys. Chem. 69 (1997) 185–198.
[24] C. Arcangeli, A.R. Bizzarri, S. Cannistraro, Concerted motion in copper plastocyanin and azurin: an essential dynamics study, Biophys. Chem. 90 (2001) 45–56.
[25] A.R. Bizzarri, S. Cannistraro, Molecular dynamics simulation evidence of anomalous diffusion of protein hydration water, Phys. Rev. E 53 (1996) 3040–3043.
[26] C. Arcangeli, A.R. Bizzarri, S. Cannistraro, MD simulation and essential dynamics study of mutated plastocyanin: structural, dynamical and functional effects of a disulphide bridge insertion at the protein surface, Biophys. Chem. 92 (2001) 183–199.
[27] J.J. Davis, D. Djuric, K.K.W. Lo, W.L.L. Wong, H.A.O. Hill, A scanning tunneling study of immobilized cytochrome P450, Faraday Discuss 116 (2000) 15–22.
[28] S.T. Tang, A.J. McGhie, Imaging individual chaperonin and immunoglobulin G molecules with scanning tunneling microscope, Langmnir 12 (1996) 1088–1093.
[29] C.L. Brooks, R.E. Bruccoleri, B.D. Olafson, D.J. Statos, S. Swaminathan, M. Karplus, CHARMM: a program for macromolccular energy, minimization, and dynamics calculations, J. Comp. Chem. 4 (1983) 187–217.
[30] A.D. MacKerrell Jr, D. Bashford, M. Bellott, R.L. Dunbrack Jr, J.D. Evanseck, M.J. Field, et al., All-atom empirical potential for molecular modeling and dynamics studies of proteins, J. Phys. Chem. B 102 (1998) 3586–3616.
[31] J.M. Guss, H.D. Bartunik, H.C. Freeman, Accuracy and precision in protein structure analysis; restrained least-squares refinement of the structure of poplar plastocy-

anin at 1.33 Å resolution, Acta Cryst. B48 (1992) 790–811.
[32] A.R. Bizzarri, S. Cannistraro, Intensity fluctuations of the copper site resonant vibrational modes as observed by MD simulation in single plastocyanin molecule, Chem. Phys. Lett. 349 (2001) 497–503.
[33] L.W. Ungar, N.F. Seherer, G.A. Voth, Classical molecular dynamics simulation of the photoinduced electron transfer dynamics of plastocyanin, Biophys. J. 72 (1997) 5–17.
[34] M.R. Redinbo, T.O. Yeates, S. Merchant, Plastocyanin: structural and functional analysis, J. Bioener. Biomembr. 26 (1994) 49–66.
[35] J.O.A. De Kerpel, U. Ryde, Protein strain in blue copper proteins studied by free energy perturbations, Proteins: Struct. Fund. Genet. 36 (1999) 157–174.
[36] P. Coniba, R. Remenyi, A new molecular mechanics force field for the oxidized form of blue copper proteins, J. Comp. Chem. 23 (2002) 697–705.
[37] P.J. Steinbach, B.R. Brooks, Protein hydration elucidated by molecular dinamics simulation, Proc. Natl. Acad. Sci. USA 90 (1993) 9135–9139.
[38] P.J. Steinbach, B.R. Brooks, Hydrated myoglobin's anharmonic fluctuations are not primarily due to dihedral transitions, Proc. Natl. Acad. Sci. USA 93 (1996) 55–59.
[39] J.P. Ryckaert, G. Ciccotti, H.J.C. Berendsen, Numerical integration of the Cartesian equations of motion of a system with constraints: molecular dynamics of *n*-alkanes, J. Comput. Phys. 23 (1977) 327–341.
[40] B. Lee, F.M. Richards, The interpretation of protein structures: estimation of static accessibility, J. Mol. Biol. 55 (1971) 379–400.
[41] D.J. Lavrich, S.M. Wetterer, S.T. Bernasek, G. Scoles, Physisorption and chemisorption of alkanethiols and alkyl sulfides on Au(111), J. Phys. Chem. B 102 (1998) 3456–3465.
[42] H.H. Jung, Y.D. Won, S. Shin, K. Kim, Molecular dynamics simulation of benzenethiolate and benzyl mercaptide on Au(111), Langmuir 15 (1999) 1147–1154.
[43] J. Qian, R. Hentschke, W. Knoll, Superstructures of cyclodextrin derivatives on Au(111): a combined random planting-molecular dynamics approach, Langmuir 13 (1997) 7092–7098.
[44] A. Amadei, A.B.M. Linssen, H.J.C. Bercndsen, Essential dynamics of proteins, Proteins: Struct. Funct. Genet. 17 (1993) 412–425.
[45] A.E. Garcia, Large amplitude nonlinear motions in proteins, Phys. Rev. Lett. 68 (1992) 2696–2699.
[46] A.R. Bizzarri, S. Cannistraro, Flickering noise in the potential energy fluctuations of proteins as investigated by MD simulation, Phys. Lett. A 236 (1997) 596–601.
[47] H. Frauenfelder, F. Parak, R.D. Young, Conformational substates in proteins, Ann. Rev. Biophys. Biophys. Chem. 17 (1988) 451–479.
[48] P.H. Hueneberger, A.E. Mark, W.F. van Gunsteren, Fluctuations and cross-correlation analysis of protein motions observed in nanosecond molecular dynamics simulations, J. Mot. Biol. 252 (1995) 492–503.
[49] H. Assender, V. Bliznyuk, K. Porfyrakis, How surface topography relates to materials' properties, Science 297 (2002) 97ex3–976.
[50] L. Andolfi, B. Bonanni, G.W. Canters, M.Ph. Verbeet, S. Cannistraro, SPM characterization of gold-chemisorbed poplar plastocyanin mutants, Surf. Sci. 530 (2003) 181–194.
[51] R.A. Marcus, N. Sutin, Electron transfer in chemistry and biology, Biochim. Biophys. Acta 811 (1985) 268–322.
[52] G.R. Loppnow, E. Fraga, Proteins as solvents: the role of amino acid composition in the excited-state charge transfer dynamics of plastocyanins, J. Am. Chem. Soc. 119 (1997) 896–905.